Retrieval of emissivity and temperature profile in polar regions

Nizy Mathew, Georg Heygster and Philip W. Rosenkranz*
Institute of Environmental Physics,University of Bremen, 28334 Bremen, Germany
Tel.:+49 421 218 4726, Fax:+49 421 218 4555, E-mail:mathew@iup.physik.uni-bremen.de
* Research Laboratory of Electronics, Massachusetts Institute of Technology, Cambridge Massachusetts, USA

Abstract – Polar regions are composed of different surface types, e.g., open water, land ice and different types of sea ice. As a consequence the retrieval of near surface atmospheric parameters (temperature, humidity etc..) is restricted due to the high and highly variable surface emissivity except for open water. The surface emissivities are retrieved using the brightness temperatures at window channels of the cross-track scanning Advanced Microwave Sounding Unit (AMSU) satellite radiometer. The emissivities are practically constant up to local zenith angles of 45°. Comparison of temperature profiles retrieved from AMSU is done with the radiosonde measurements. The root mean square deviations from the measurements is 2 K. Near the surface it increases up to 6 K.

I. INTRODUCTION

Polar regions play an important role in the global climate. Knowledge of temperature profiles is vital in climatological and meteorological studies and numerical weather prediction. Data from the satellite borne radiometer AMSU on the National Oceanic and Atmospheric Administration (NOAA) satellites are well suited for the temperature profile retrieval [1].

Quantitative knowledge of the spatial and temporal variability of surface emissivity for all the window channels and for all scan angles is essential for the retrieval of atmospheric parameters with improved accuracy in the lower troposphere over polar regions. In the present study a method to retrieve the emissivity is applied over the polar regions, irrespective of surface types or seasonal variability. AMSU data from NOAA-15 satellites are used here.

Polar temperature profiles are retrieved from NOAA-16 AMSU data using a radiative transfer algorithm and the results are compared with the collocated radiosonde observations. The retrieval errors are quantified.

II. SURFACE EMISSIVITY

A. Data and Model

The passive microwave radiometers AMSU on the new generation NOAA polar orbiting satellite consists of two modules 'A' and 'B'. The AMSU-A has 15 channels in the frequency range 23 - 89 GHz, with window channels at 23.8, 31.4, 50.3 and 89 GHz. The instrument has an instantaneous field of view (IFOV) of 3.3° at half power points, which provides a spatial resolution of 48 km at nadir. There are 30 measurements on each scan line. The AMSU-B has five channels in the frequency range 89 - 183 GHz with 90 measurements on each scan line. The IFOV of AMSU-B is 1.1° and the spatial resolution at nadir is about 16 km [2]. The channels at 89 GHz and 150 GHz are window channels. The retrieval of surface emissivity is most accurate for window channels since these measurements are least affected by the atmospheric absorption and emission. The satellite has an orbital inclination of 98°, and the swath width is around 2068 km. This results in the coverage of high latitudes only with the right-hand high scan angle portions of the swath.

The atmospheric contribution to the brightness temperature measurement of satellite is eliminated by radiative transfer simulations using the radiative transfer model MWMOD (MicroWave radiative transfer MODel) [3]. For the polar regions, in situ measurements from radiosondes are sparse, especially atmospheric profiles over sea ice. We use ECMWF data in a 1.5° grid having 60 vertical levels as the atmospheric profiles. The profiles are available globally, in every 6 hours.

B. Method

The total brightness temperature measured by the satellite can be written as

$$\begin{aligned} T_b &= T_u(\nu,\theta) + \varepsilon(\nu,\theta) T_s \mathrm{e}^{-\tau \sec\theta} \\ &\quad + (1-\varepsilon(\nu,\theta)) T_d(\nu,\theta) \mathrm{e}^{-\tau \sec\theta} \end{aligned} \tag{1}$$

where $T_u(\nu,\theta)$ is the up-welling radiation from the atmosphere, T_s is the physical temperature of the surface, ε is the emissivity of the surface, $T_d(\nu,\theta)$ is the down-welling radiation, τ is the total atmospheric opacity and ν and θ are the observing frequency and incidence angle respectively. (1) can be rearranged as the equation for emissivity [4]

$$\varepsilon(\nu,\theta) = \frac{T_b - T_b(\varepsilon=0)}{T_b(\varepsilon=1) - T_b(\varepsilon=0)} \tag{2}$$

where T_b is the brightness temperature measured by the satellite for a particular frequency and zenith angle, $T_b(\varepsilon=0)$ and $T_b(\varepsilon=1)$ are simulated brightness temperatures with $\varepsilon=0$ and $\varepsilon=1$ respectively and are determined from known atmospheric profiles.

C. Results

The AMSU instruments measure in a mixed linear polarization mode. If θ_s is the scan angle and θ is the local

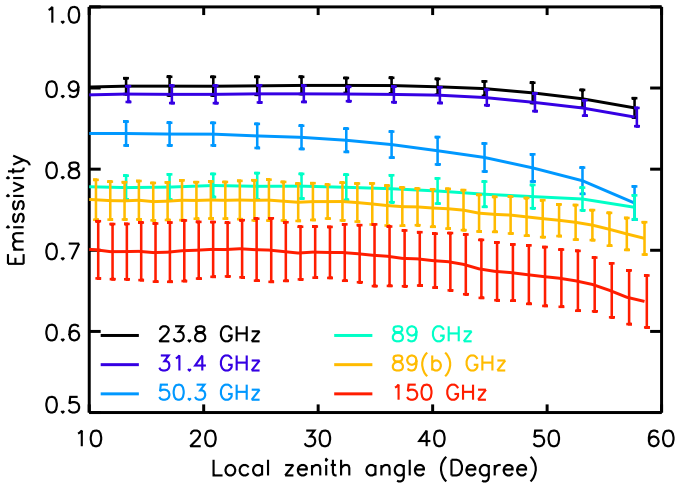

Fig. 1. The variation of emissivity of first-year ice in the Kara sea region (76.5°N-78°N and 77°-79°E) in the Arctic for March 2005 with local zenith angles for different frequencies. The error bars represent standard deviation.

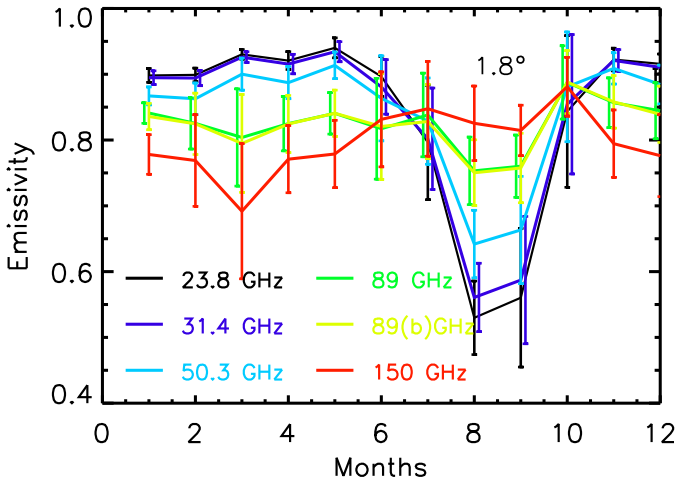

Fig. 2. The seasonal variation of emissivity of small region in Kara sea in the Arctic for the year 2002 for different frequencies and for local zenith angle of 1.8°. The error bars represent standard deviation.

zenith angle, then the surface emissivity ε for AMSU window channels can be written as

$$\varepsilon(\theta) = \varepsilon_v(\theta)\cos^2(\theta_s) + \varepsilon_h(\theta)\sin^2(\theta_s) \qquad (3)$$

where ε_v and ε_h are the vertically and horizontally polarized surface emissivities respectively [5]. In general (for plane Fresnel emissivities and more realistic emissivity models), ε_v increases with incidence angles while ε_h decreases, this compensates the decreasing of cosine square and the increasing of sine square.

A small region is selected in the Kara sea (76.5°-78°N and 77°-79°E) usually covered with first year ice during the Arctic winter months. In (2), the term $T_b(\epsilon = 1)$ contains also the temperature of the emitting layer T_s. As setting it equal to the temperature of the lowest atmospheric level T_a leads to un-physically high emissivities (sometimes exceeding 1) we estimate T_s from data of the field campaign ARKTIS'93 where similar lower atmospheric temperatures prevailed and where both atmospheric and sea ice temperature profiles were taken [7]. From this sea ice temperature profile and the penetration depths varying in the frequency range of 23 and 89 GHz between 13 and 3 cm [8] we conclude as a rough estimate $T_s = T_a + 20\ K$. Fig. 1 represents the angular variation of the average emissivity of March 2005. Different colors indicate different frequencies. The emissivity decreases with frequency. The dependence on the incidence angle is low up to about 45°, beyond that it decreases strongly. This behavior is more pronounced with increasing frequency. It can easily be understood from the discussion of (3). The sensitivity to atmospheric parameters increases with frequency, and so does the observed variability because of the inevitable errors in the model atmospheric profiles. The variability (standard deviation) of emissivity is indicated by error bars.

The seasonal variation of the surface emissivity is studied in the Kara sea for the year 2002. In this region, there is first year ice during Arctic winter months and open water during

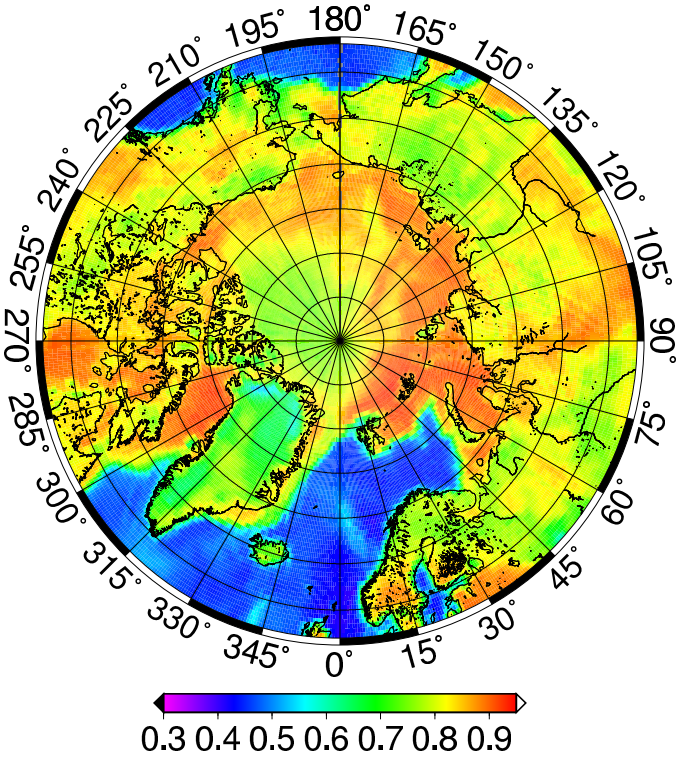

Fig. 3. Emissivity map of arctic for 02/04/2002 at 23.8 GHz

the rest of the year. The variation of frequency dependence of emissivity (emissivity decreases with frequency for sea ice and increase in emissivity for increase in frequency for open water) for different seasons can be clearly seen in Fig. 2.

Fig. 3 shows a daily average emissivity map of the Arctic at 23.8 GHz on 02/04/2002. All AMSU over passes matching in time and space are used for the map irrespective of the local zenith angles. Its plotted at resolution 0.5°. From the map, it is possible to distinguish different surfaces, e.g., low emissivity region as open ocean, high emissivity regions as land and the moderate emissivity region as sea ice. Note that

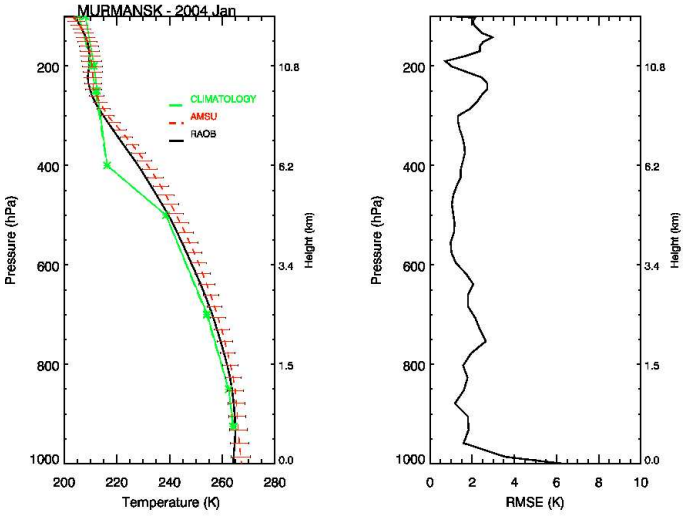

Fig. 4. Comparison of the retrieved temperature profiles with the radiosonde measurements.The error bars represent standard deviation.

the emissivity value is quantitatively only valid for sea ice. In the open water and land regions the estimates of penetration depth and temperature profile within the surface do no longer hold. These values are only shown for reference.

III. TEMPERATURE PROFILES

Temperature profiles are retrieved using an algorithm [6] developed for AIRS/AMSU/HSB, and adapted for use with NOAA-16 AMSU-A/B. A forward radiative transfer model is used to calculate microwave brightness temperatures. Components of the microwave model include a surface emissivity model, the influence of surface scattering characteristics on reflected down-welling emission from the atmosphere and an atmospheric transmittance model.

The retrieved temperature profiles are compared with measurements made by different stations in the polar regions. Radiosonde stations in polar regions are mostly located near coastlines where surface type and emissivity might change within the sensor footprint. Fig. 4 shows a sample comparison of AMSU retrieved temperature profiles with the collocated radiosonde observation for the station Murmansk (68°58'N 33°03'E) for the month January 2004 and also the root mean square difference between the retrieved profiles and the radiosonde temperature profiles. Collocations are done within a time window of ± 3 hours and space window of ± 100 km. Error bars represent standard deviation. Large deviations are observed near the surface.

The suitability of ECMWF model profiles instead of those from radiosondes for the comparison with AMSU retrieved temperature profiles is demonstrated in Fig. 5. Three profiles, obtained from a research expedition conducted in the Baltic Sea in 2001 February, which are not assimilated into ECMWF model have been compared with collocated ECMWF profiles and retrieved temperature profiles from AMSU. The error bars indicate the standard deviation. The ECMWF model profiles show good agreement with radiosonde measurements, however AMSU profiles show deviations, especially near the surface. A possible reason for the deviations of profiles in the Baltic area, or indeed any location close to a coastline, is the simplified estimate of the land fraction within the AMSU-A footprint, which is set either to 0 or 1 according to the surface elevation at the center of the footprint; this is a difference from the version of the algorithm in [6]. Therefore the forward calculation may be starting with an a-priori surface emissivity that is very different from the average over the AMSU-A footprint. In order to study the temperature profile variation with emissivity variation over sea ice, in-situ observations with homogeneous surface type within the sensor footprint, e.g., from research vessels are still required.

IV. CONCLUSIONS

Surface emissivities are calculated in the polar region at AMSU frequencies. Emissivity maps were produced to see the emissivity variation for different surface types of polar regions. The variation of emissivities with incidence angle can be neglected up to $\pm 45°$ corresponding to scan positions 4 to 27 for AMSU-A and 10 to 81 for AMSU-B. The retrieved temperatures profiles are compared with the in-situ measurements and the root mean square difference between the retrieved and in-situ measured profiles are calculated. The comparison in Fig. 5 shows that ECMWF model profiles are well suited to validate AMSU profiles. We intend to improve the near surface part by including a priori knowledge about the emissivities into the retrieval.

ACKNOWLEDGEMENTS

This work was funded by DFG grant He 1746/9-1,2,3.

REFERENCES

[1] Rosenkranz, P.W.: Retrieval of Temperature and Moisture Profiles From AMSU-A and AMSU-B Measurements; *IEEE Trans. Geosci. Rem. Sens.*, vol. 39, NO. 11, pp2429-2435, Nov. 2001

[2] Goodrum, G., Kidwell, K. B., and Winston, W.: NOAA KLM USER'S GUIDE; *U.S. Department of Commerce, National Oceanic and Atmospheric Administration*, 2000

[3] Fuhrhop, R., Grenfell, T.C., Heygster, G., Johnson, K., Schüsseland P., Schrader, M., and Simmer C.; A combined radiative transfer model for sea ice, open ocean and atmosphere, *Radio Sci.*, vol.33, NO. 2, pp303-316, March-April 1998

[4] Felde, G.W., Pickle, J.D.; Retrieval of 91 and 150 GHz Earth surface emissivities, *J. Geophys. Res.*, vol. 100, NO. D10, pp20,855-20,866, October 1995

[5] Weng, F., Zhao, L., Ferraro, R.R., Poe, G., Li, X., and Grody, N.C.; Advanced microwave sounding unit cloud and precipitation algorithms, *Radio Sci.*, vol. 38, NO. 4, ppMAR 33-1 - MAR 33-13, 2003

[6] Rosenkranz, P.W., Barnet, C.D.; Microwave radiative transfer model validation, *J. Geophys. Res.*, vol. 111, D09S07, doi:10.1029/2005JD006008, 2006

[7] Fuhrhop, R., Simmer, C., Schrader, M., Heygster, G., Johnson, K., and Schüssel, P.; Study of Passive Remote Sensing of the Atmosphere and Surface Ice, Berichte aus dem Institut für Meereskunde, No. 297, Kiel, 1997

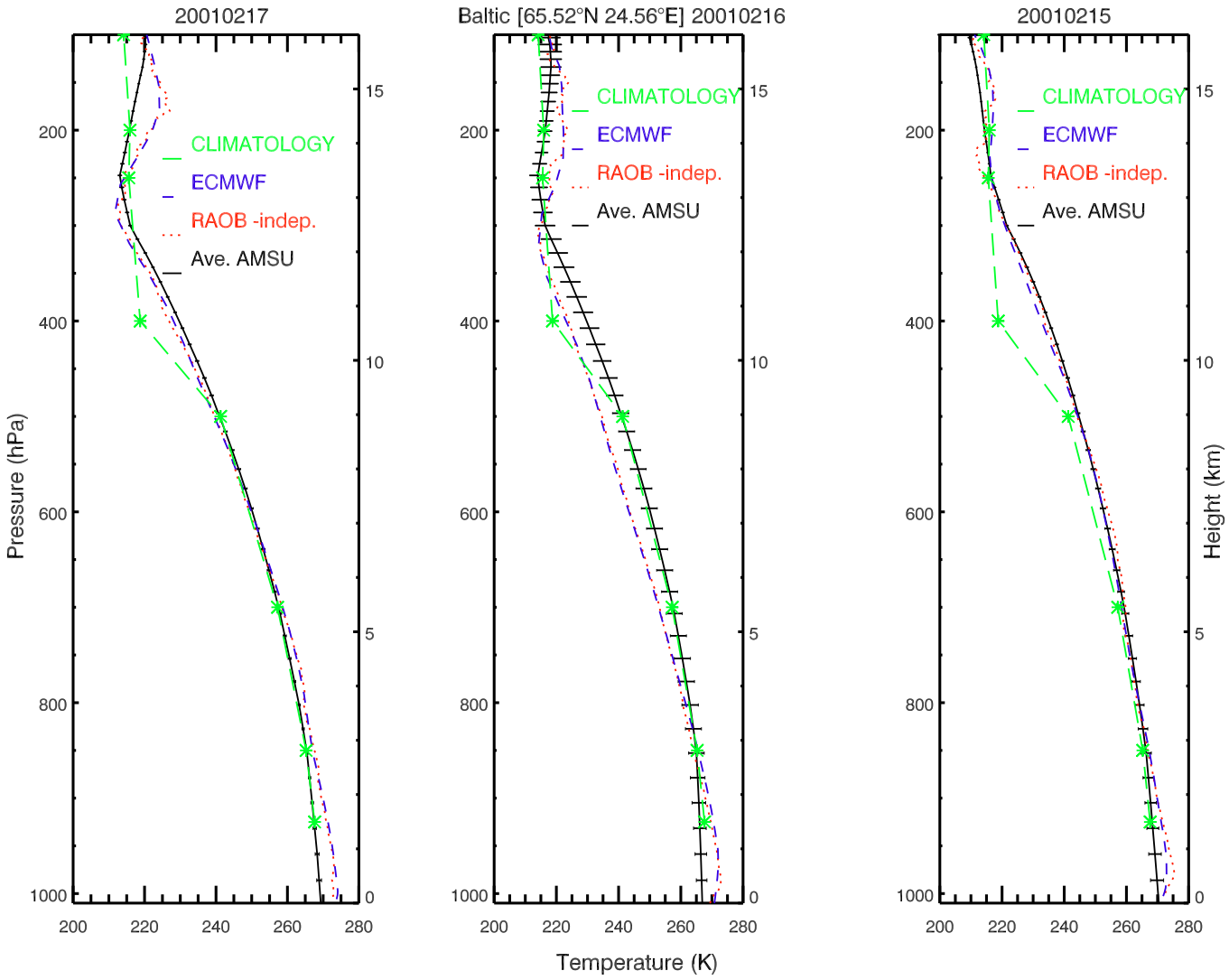

Fig. 5. Comparison of temperature profiles from different sources.The error bars represent standard deviation.

[8] Haggerty, J. A. and Curry, J. A.; Variability of sea ice emissivity estimated from airborne passive microwave measurements during FIRE SHEBA, *J. Geophys. Res.*, vol. 106, No. D14, pp15265-15277, 2001